Journal of Materials Chemistry A

Accepted Manuscript

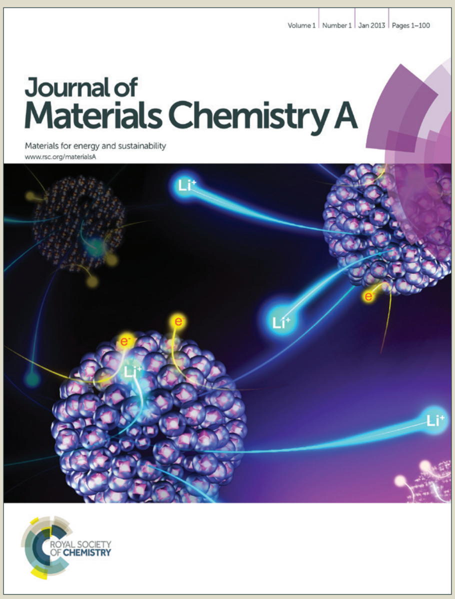

ROYAL SOCIETY OF CHEMISTRY

www.rsc.org/materialsA

Cite this: DOI: 10.1039/c0xx00000x

www.rsc.org/xxxxxx

ARTICLE TYPE

Highly stable and flexible Li-ion battery anodes based on TiO_2 coated 3D carbon nanostructures

Xing Hui Wang,[a] Cao Guan,[b] Lei Meng Sun,[a] Rahmat Agung Susantyoko,[a] Hong Jin Fan,*[b] and Qing Zhang*[a]

Received (in XXX, XXX) Xth XXXXXXXXX 20XX, Accepted Xth XXXXXXXXX 20XX
DOI: 10.1039/b000000x

A hierarchical three dimensional carbon nanowire arrays on carbon cloth is developed as an efficient flexible nanostructure current collector for TiO_2 based anodes. This unique electrode exhibits not only ~300 times higher mass loading than that of 2D planar substrate, but also high reversible capacity, remarkable rate capability and cycling stability (up to 8000 cycles).

There is currently a great interest in development of flexible Li-ion batteries (LIBs) for soft portable electronic devices, such as rollup displays and wearable devices.[1-5] On one hand, similar to conventional hard LIBs, it is essential to develop flexible LIBs with a high capacity, high rate capability and excellent cycle life that enable electronic devices to be continuously powered for a long period of time. On the other hand, a flexible LIB must be capable of accommodating frequent large mechanical strains (e.g. bending, twisting or deforming).[6] Yet, many potential flexible LIB anodes show an insufficient rate capability, short cycle life and weak mechanical flexibility. The development of fast, highly stable LIB anodes with robust mechanical flexibility is thus highly desirable for advanced soft LIBs.

Titanium dioxide (TiO_2) has been considered as a promising anode for LIBs owing to low cost, environmental benignity and intrinsic safety.[6-11] However, the poor ionic and electronic conductivity of TiO_2 results in an insufficient Li storage performance, especially at high discharge/charge rates.[8, 10] The common and useful strategy to address this issue is to reduce transport path lengths for electrons and Li ions using TiO_2 nanostructures or combining them with highly conductive materials to yield a hybrid nanostructure.[10, 12, 13] Nevertheless, for these powder-like TiO_2 nanostructures, the electrodes are typically fabricated through mixing active materials with conductive carbon additives and polymer binders, and then casting the mixture onto a piece of two dimensional (2D) Cu foil. This type of the electrodes has several drawbacks for flexible LIBs. The additives introduce extra processing steps and also compromise the overall specific energy density.[14] In addition, the active materials may easily peel off from the Cu foils when they are bent due to insufficient adhesion. Moreover, metallic current collectors are difficult to restore their original shapes after being deformed. Very recently, integrated electrodes, where self-supported active nanomaterials are grown directly on flexible substrates, such as carbon cloth (CC) and carbon nanotube/graphene papers, have been demonstrated for flexible LIBs to overcome the above drawbacks.[6, 15-18] Among various conductive carbon substrates, CC with a high electrical conductivity and mechanical flexibility is an ideal flexible substrate.[17, 19-21] However, most CC is constructed with carbon fiber with an average diameter of ~10 μm, resulting in a relative small loading area for active materials. In addition, the thickness of active materials layers is limited to ensure short transport path lengths for electrons and Li ions for a high rate capability. These constraints cause a low mass loading density of the active materials. Therefore, it is challenging to obtain a self-supported electrode with a high mass loading density, fast charging rate and high stability for flexible LIBs.

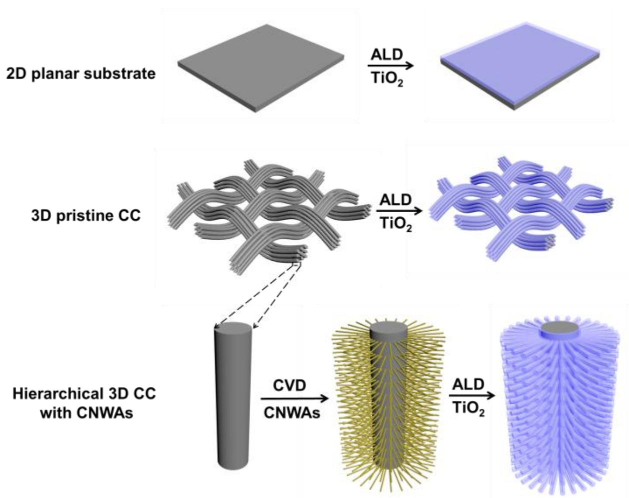

Fig. 1 Schematic comparison and fabrication processes of TiO_2 coating on 2D planar substrate (first row), 3D pristine CC (second row), and hierarchical 3D CC with CNWAs (third row).

In this work, we grow hierarchical three dimensional (3D) carbon nanowire arrays (CNWAs) on CC to actualize self-supported TiO_2 based electrode with both high mass loading density and excellent Li storage performances. As shown in Fig. 1, beneficial from the higher loading area, the mass loading density of TiO_2 for hierarchical 3D CC with CNWAs is found to be ~10 times higher than that on 3D pristine CC and ~300 times higher than that on a 2D planar substrate. When used as a binder-free anode for LIBs, the as-synthesized hierarchical 3D C@TiO_2 core-shell nanocable arrays (NCAs) electrode displays a high reversible capacity (a reversible capability of 309 mAh g^{-1} at 0.2 C), a remarkable rate capability (a reversible capability of 100 and 47 mAh g^{-1} at 20 and 50 C, respectively), and a superior long term cycling stability (a high reversible capacity of 170 mAh g^{-1} after 8000 cycles at 10 C with only 0.0019% capacity decay per cycle).

The synthesis strategy of hierarchical 3D C@TiO_2 core-shell NCAs on CC is schematically illustrated in Fig. 1. First, CNWAs were grown on CC in a thermal chemical vapor deposition (TCVD) tube furnace using Fe and C_2H_2 as catalyst and carbon source, respectively. The typical morphologies of the as-synthesized CNWAs on CC were shown in Fig. S1, revealing that the carbon nanowires are uniformly grown on CC with an average diameter of ~52 nm. TiO_2 was conformally coated on the scaffold of the carbon nanowires using the atomic layer deposition (ALD) technique which can not only precisely control thin film deposition at the Ångstrom-level, but also deposit conformal thin films on high aspect ratio substrates.[8] As shown in Fig. 2, TiO_2 coating was found to be very uniform, and no uncoated carbon nanowires can be seen after the deposition. The inset of Fig. 2a shows that the CC maintains its flexibility after C@TiO_2 core-shell NCAs growth. The close observation (Fig. 2d) reveals that an individual TiO_2 coated carbon nanowires were typically with an average outer diameter of ∼125 nm, indicating that the thickness of the coated TiO_2 thickness is ∼36.5 nm. In addition, the side view SEM image of single carbon microfiber (Fig. 2e) verifies that the C@TiO_2 nanocables with a length of about 5-10 μm were radially grown all around the carbon microfibers. Fig. 2f further confirms that even the root of the carbon nanowires were uniformly coated with TiO_2 as indicated by the white dash arrows.

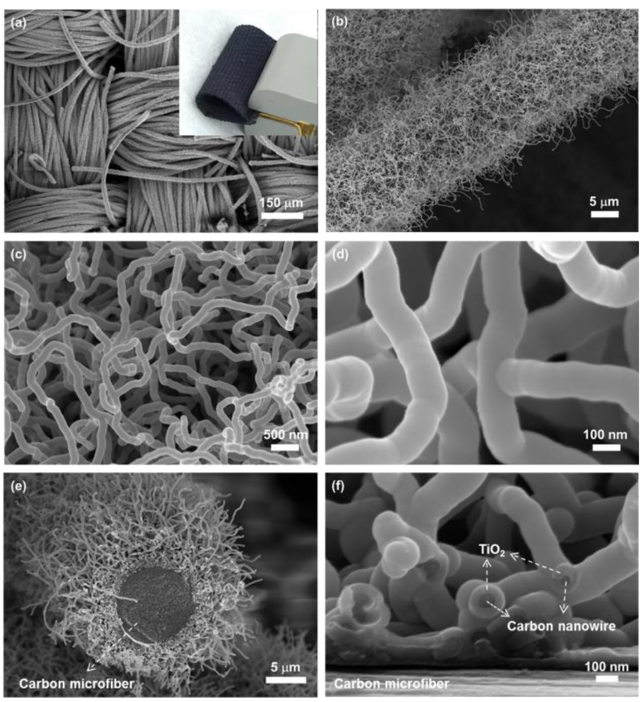

Fig. 2 Morphology characterization of the hierarchical 3D C@TiO_2 core-shell NCAs. (a and b) The low magnification and (c and d) high magnification top view SEM images of the C@TiO_2 core-shell NCAs. The inset in (a) shows a piece of flexible carbon cloth after the C@TiO_2 core-shell NCAs growth. (e) The low magnification side view SEM image of the C@TiO_2 core-shell NCAs on a single microfiber. (f) High magnification side view SEM image of the root of the C@TiO_2 core-shell NCAs.

Further morphological and structural characterizations of the C@TiO_2 core-shell NCAs were performed using transmission electron microscopy (TEM). Fig. 3a shows the TEM image of an individual C@TiO_2 nanocable, indicating that uniform TiO_2 coating was achieved over carbon nanowires. The coaxial core-shell structure of carbon nanowire and TiO_2 can be well distinguished from the gray scale contrast in high resolution TEM image (Fig. 3b). The thickness of TiO_2 coating is observed to be around 35 nm by TEM, in good agreement with the result measured in SEM. The energy-dispersive X-ray spectrometry (EDS) mapping analysis was further employed and shown in Fig. 3c-f. The uniform elemental distribution and core-shell structure of C@TiO_2 were confirmed by Ti and O signal peaks at the outside (shell) of the composite nanocable and C signal peak at the inner part (core) of the cable. In addition, no crystalline planes and diffraction features were seen from the TiO_2 layer (Fig. S2), suggesting that coated TiO_2 maintained an amorphous phase, which could be beneficial for higher rate capability in comparison with the crystalline phase of TiO_2.[22]

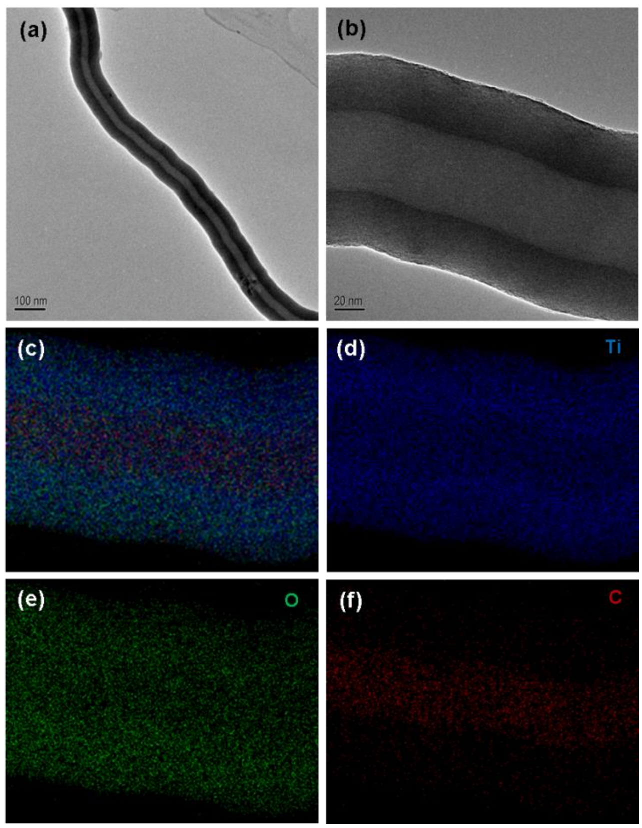

Fig. 3 Morphology characterization of single C@TiO_2 core-shell nanocable. (a) The TEM and (b) HRTEM image of a C@TiO_2 core-shell nanocable. (c) The corresponding EDX elemental mappings overlaps of (d) Ti, (e) O, and (f) C for the C@TiO_2 core-shell nanocable.

The Li storage performance of the hierarchical 3D C@TiO_2 core-shell NCAs were evaluated by directly using them as a self-supported electrode in a coin cell configuration with Li as the counter electrode. Fig. 4a shows the initial three voltage profiles of hierarchical 3D C@TiO_2 core-shell NCAs electrode at a current rate of 0.2 C (1 C = 335 mA g^{-1}) in the voltage range of 1-3 V (vs. Li^+/Li). It can be seen that the voltage decreased and increased progressively versus capacity during discharge (lithiation) and charge (delithiation) process, respectively, showing the typical sloping behavior of amorphous TiO_2.[8, 22] The initial discharge and charge capacities were found to be 351 and 241 mAh g^{-1}, respectively, yielding an initial Coulombic efficiency (CE) of 68.7%. The irreversible capacity loss in the first cycle could be mainly attributed to the irreversible Li ion insertion into TiO_2 and the interfacial reaction between the electrolyte and TiO_2, which is common to most anode materials.[6, 8, 23-25] After first three cycles at 0.2 C, the capacity retention of the electrode was then tested at 1C for subsequent 200 cycles. As shown in Fig. 4b, the hierarchical 3D C@TiO_2 core-shell NCAs electrode exhibits a good cycling stability. Although the capacity increased slightly in the first 80 cycles, it stabilized at around 228 mAh g^{-1} in the following 120 cycles. The initial increasing capacity is probably caused by more reacting sites being activated with increasing cycle numbers, participating in the Li ion storage and contributing to the capacity.[26] Interestingly, although the thickness of coated TiO_2 was only 35 nm (500 ALD cycles), the mass loading density of the TiO_2 in hierarchical 3D C@TiO_2 core-shell NCAs electrode was as high as 4.0 mg cm^{-2}, much higher than most reported integrated electrodes.[6, 9, 25, 27-30] In comparison, it is only 0.4 and 0.013 mg cm^{-2} for the same thick TiO_2 coating on 3D pristine CC and 2D planar substrate, respectively. In other words, the hierarchical 3D C@TiO_2 core-shell NCAs electrode exhibited ~10 and ~300 times higher mass loading density than that for 3D pristine CC and traditional 2D planar substrates, respectively.

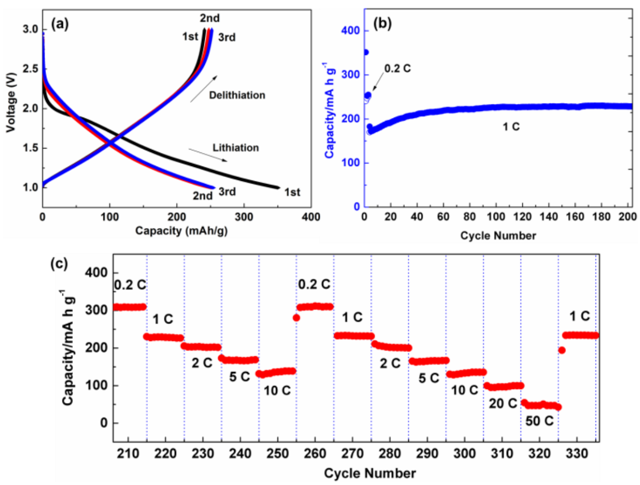

Fig. 4 Electrochemical performance of hierarchical 3D C@TiO_2 core-shell NCAs electrode. (a) The initial three voltage profiles at a rate of 0.2 C. (b) The capacity retention at 0.2 C for initial three cycles and then 1 C for subsequent 200 cycles. (c) Rate capability at various C rates from 0.2 to 50 C.

After 200 cycles at 1 C rate, the rate capability of the electrode was examined at different current rates ranging from 0.2 to 50 C. As shown in Fig. 4c, the capacities were quite stable at each rate. The electrode could yield a high capacity of 309 mAh g^{-1} (1.236 mAh cm^{-2}) at a low rate of 0.2 C in 213th cycle, which is much higher than the capacity of commercialized $Li_4Ti_5O_{12}$ anode (~175 mAh g^{-1}) and anatase TiO_2 (~167 mAh g^{-1}).[8] Then the discharge capacities of 226, 202, 169, 139, 100 and 47 mAh g^{-1} were obtained when cycled at high rates of 1, 2, 5, 10, 20 and 50 C, respectively. More importantly, the electrode could recover 100% of its capacity when the rates reduced back to the initial rate of 0.2 or 1 C after various high rate cycling. These results show that the hierarchical 3D C@TiO_2 core-shell NCAs electrode exhibited an excellent rate capability.

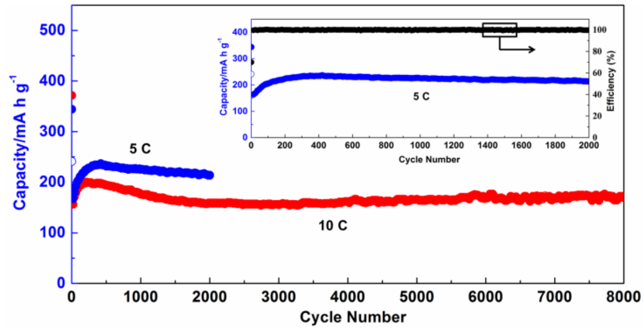

Fig. 5 Long term capacity retention of hierarchical 3D C@TiO_2 core-shell NCAs electrode at a rate of 5 (blue) and 10 C (red). Inset shows the capacity retention and CE at a rate of 5 C.

In order to further demonstrate the long term cycling stability of the hierarchical 3D C@TiO_2 core-shell NCAs electrode, the cells were measured under high rates of 5 and 10 C for up to 2000 and 8000 cycles, respectively, as shown in Fig. 5. After the first three cycles at the low rate of 0.2 C, an initial discharge capacity of 154 mAh g^{-1} was achieved at a high rate of 5 C (Fig. 5). Then the capacity gradually increased and then stabilized at a high value of 214 mAh g^{-1} even after 2000 cycles, corresponding to a capacity retention of 91.1% of the highest capacity. Moreover, the CE value for each cycle (right axis in the inset of Fig. 5) maintained at above 99.7% except the initial several cycles. When the current rate was increased to 10 C, a high capacity of 170 mA h g^{-1} could be obtained even over 8000 cycles. The overall capacity decay was as low as 0.0019% per cycle. These results suggest that the hierarchical 3D C@TiO_2 core-shell NCAs electrode possessed excellent tolerance of fast insertion and extraction of Li ions for long lifespan LIBs. We further assembled a whole flexible LIB using the C@TiO_2 core-shell NCAs anode and commercial $LiMn_2O_4$ cathode. The packaged whole flexible battery is bendable and foldable with high mechanical flexibility and stability. It can be fully charged to 3.5 V and is able to light a LED no matter if it was in a flat (Fig. 6a) or folded (Fig. 6b) states. More details have been added in Supplementary Video S1. The typical voltage plateau and capacity retention of C@TiO_2/$LiMn_2O_4$ whole battery at a current rate of 5 C in the voltage range of 1-3.5 V were shown in Fig. S3. A high reversible discharge capacity of 223 mA h g^{-1} was obtained after 1000 cycles at a high rate of 5 C, corresponding to a high energy density of 481.5 W h kg^{-1} based on the mass of the TiO_2. These results suggest that the hierarchical 3D C@TiO_2 core-shell NCAs electrode could possess an excellent stability in flexible whole batteries.

To further examine the structure change of hierarchical 3D C@TiO_2 core-shell NCAs, the electrode was disassembled after 2000 cycles at a high rate of 5 C. As shown in Fig. S4, their original textural properties in terms of shape, size and structural integrity were well maintained, demonstrating a high structural stability of the composite core-shell NCAs under fast discharge/charge cycles. Therefore, the remarkable Li storage performance of hierarchical 3D C@TiO_2 core-shell NCAs electrode should result from the following merits: First, the C@TiO_2 nanocable structure greatly shortens the ionic diffusion length and provides sufficient electrode-electrolyte contact area for Li^+ insertion and extraction reactions.[6, 26] Second, carbon nanowires grown directly on carbon microfiber play an important role in enhancing electrode conductivity through forming a continuous electronic path for fast and stable electron transfer while granting the electrode with high loading area for high mass loading density.[31, 32] Third, TiO_2 coating grew firmly on carbon nanowires to maintain the structural integrity under fast and long term cycling. In addition, we would point out that the mass loading density of TiO_2 in hierarchical 3D C@TiO_2 core-shell NCAs electrode can be further increased to be ~7.0 mg cm^{-2} through increasing TiO_2 layer thickness up to ~60 nm. As shown in Fig. S5, the electrode with such high mass loading could also demonstrate excellent capacity retention, which is beneficial for high energy density.

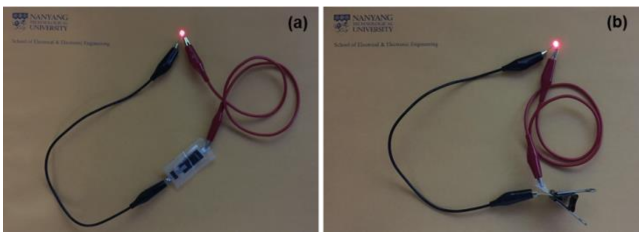

Fig. 6 Optical photographs of a red LED lightened by the flexible whole battery under flat (a) and fold (b) states.

Conclusions

Hierarchical 3D C@TiO_2 core-shell NCAs on carbon cloth have been developed as an efficient anode electrode for flexible LIBs. The hierarchical 3D carbon based nanostructured electrode dramatically increases the mass loading density of TiO_2 coating in comparison with 3D pristine CC and traditional 2D planar substrates. Owing to the shortened Li^+ diffusion length, high contact surface area, high electronic conductivity and good structural stability, hierarchical 3D C@TiO_2 core-shell NCAs electrode exhibits a high reversible capacity, remarkable rate capability and superior long term cycling stability. We envision that this hierarchical nanostructure design concept holds a great promise for development of flexible LIBs and supercapacitors with high power and energy densities.

Acknowledgements

The project was financially supported by MOE AcRF Tier2 Funding, Singapore (MOE2011-T2-1-137 and MOE 2013-T2-2-100). H.J. Fan thanks the support from SERC Public Sector Research Funding (Grant number 1121202012), Agency for Science, Technology, and Research (A*STAR).

Notes and references

[a] *NOVITAS, Nanoelectronics Centre of Excellence, School of Electrical and Electronic Engineering, Nanyang Technological University, Singapore 639798, Singapore; E-mail: eqzhang@ntu.edu.sg*

[b] *School of Physical and Mathematical Sciences, Nanyang Technological University, Singapore 637371, Singapore, E-mail: fanhj@ntu.edu.sg*

† Electronic Supplementary Information (ESI) available: Experiments section, SEM and TEM images of the hierarchical 3D carbon nanowire arrays on carbon cloth, SEM images of the hierarchical 3D C@TiO_2 core-shell NCAs after 2000 cycles at a high rate of 5 C are given in the supporting information. See DOI: 10.1039/b000000x/

‡ Footnotes should appear here. These might include comments relevant to but not central to the matter under discussion, limited experimental and spectral data, and crystallographic data.

1. H. Nishide and K. Oyaizu, *Science*, 2008, **319**, 737-738.
2. M.-H. Park, M. Noh, S. Lee, M. Ko, S. Chae, S. Sim, S. Choi, H. Kim, H. Nam, S. Park and J. Cho, *Nano Lett.*, 2014, **14**, 4083-4089.
3. X. Wang, X. Lu, B. Liu, D. Chen, Y. Tong and G. Shen, *Adv Mater*, 2014, **26**, 4763-4782.
4. Q. Xiao, Q. Zhang, Y. Fan, X. Wang and R. A. Susantyoko, *Energ Environ Sci*, 2014, **7**, 2261-2268.
5. N. Li, Z. Chen, W. Ren, F. Li and H.-M. Cheng, *Proceedings of the National Academy of Sciences*, 2012, **109**, 17360-17365.
6. S. Liu, Z. Wang, C. Yu, H. B. Wu, G. Wang, Q. Dong, J. Qiu, A. Eychmüller and X. W. Lou, *Adv Mater*, 2013, **25**, 3462-3467.
7. J. Liu, K. Song, P. A. van Aken, J. Maier and Y. Yu, *Nano Lett.*, 2014, **14**, 2597-2603.
8. C. Ban, M. Xie, X. Sun, J. J. Travis, G. Wang, H. Sun, A. C. Dillon, J. Lian and S. M. George, *Nanotechnology*, 2013, **24**, 424002.
9. Y. Tang, Y. Zhang, J. Deng, J. Wei, H. L. Tam, B. K. Chandran, Z. Dong, Z. Chen and X. Chen, *Adv Mater*, 2014, **26**, 6111-6118.
10. B. Wang, H. Xin, X. Li, J. Cheng, G. Yang and F. Nie, *Sci. Rep.*, 2014, **4**, 3729.
11. C. Zhu, X. Xia, J. Liu, Z. Fan, D. Chao, H. Zhang and H. J. Fan, *Nano Energy*, 2014, **4**, 105-112.
12. S. Brutti, V. Gentili, H. Menard, B. Scrosati and P. G. Bruce, *Adv Energy Mater*, 2012, **2**, 322-327.
13. D. Wang, D. Choi, J. Li, Z. Yang, Z. Nie, R. Kou, D. Hu, C. Wang, L. V. Saraf, J. Zhang, I. A. Aksay and J. Liu, *ACS Nano*, 2009, **3**, 907-914.
14. D. Liu and G. Cao, *Energ Environ Sci*, 2010, **3**, 1218-1237.
15. G. Zhou, F. Li and H.-M. Cheng, *Energ Environ Sci*, 2014, **7**, 1307-1338.
16. L. Hu, H. Wu, F. La Mantia, Y. Yang and Y. Cui, *ACS Nano*, 2010, **4**, 5843-5848.
17. B. Liu, J. Zhang, X. Wang, G. Chen, D. Chen, C. Zhou and G. Shen, *Nano Lett.*, 2012, **12**, 3005-3011.
18. J. Chen, J. Z. Wang, A. I. Minett, Y. Liu, C. Lynam, H. Liu and G. G. Wallace, *Energ Environ Sci*, 2009, **2**, 393-396.
19. L. Shen, B. Ding, P. Nie, G. Cao and X. Zhang, *Adv Energy Mater*, 2013, **3**, 1484-1489.
20. W. Ren, C. Wang, L. Lu, D. Li, C. Cheng and J. Liu, *Journal of Materials Chemistry A*, 2013, **1**, 13433-13438.
21. C. Guan, X. Wang, Q. Zhang, Z. Fan, H. Zhang and H. J. Fan, *Nano Lett.*, 2014, **14**, 4852-4858.
22. H.-T. Fang, M. Liu, D.-W. Wang, T. Sun, D.-S. Guan, F. Li, J. Zhou, T.-K. Sham and H.-M. Cheng, *Nanotechnology*, 2009, **20**, 225701.
23. X. Wang, R. A. Susantyoko, Y. Fan, L. Sun, Q. Xiao and Q. Zhang, *Small*, 2014, **10**, 2826-2829.
24. W. J. H. Borghols, D. Lützenkirchen-Hecht, U. Haake, W. Chan, U. Lafont, E. M. Kelder, E. R. H. van Eck, A. P. M. Kentgens, F. M. Mulder and M. Wagemaker, *J. Electrochem. Soc.*, 2010, **157**, A582-A588.
25. X. Wang, L. Sun, R. Agung Susantyoko, Y. Fan and Q. Zhang, *Nano Energy*, 2014, **8**, 71-77.
26. Y. Luo, J. Luo, J. Jiang, W. Zhou, H. Yang, X. Qi, H. Zhang, H. J. Fan, D. Y. W. Yu, C. M. Li and T. Yu, *Energ Environ Sci*, 2012, **5**, 6559-6566.
27. J. Cheng, B. Wang, H. L. Xin, C. Kim, F. Nie, X. Li, G. Yang and H. Huang, *Journal of Materials Chemistry A*, 2014, **2**, 2701-2707.

28. T. Hu, X. Sun, H. Sun, M. Yu, F. Lu, C. Liu and J. Lian, *Carbon*, 2013, **51**, 322-326.
29. J.-Y. Liao and A. Manthiram, *Adv Energy Mater*, 2014, **4**, DOI: 10.1002/aenm.201400403.
30. X. Wang, L. Qiao, X. Sun, X. Li, D. Hu, Q. Zhang and D. He, *J. Mater. Chem. A*, 2013, **1**, 4173-4176.
31. A. L. M. Reddy, M. M. Shaijumon, S. R. Gowda and P. M. Ajayan, *Nano Lett.*, 2009, **9**, 1002-1006.
32. X. Chen, H. Zhu, Y.-C. Chen, Y. Shang, A. Cao, L. Hu and G. W. Rubloff, *ACS Nano*, 2012, **6**, 7948-7955.